

Crystal structure and dielectric properties of $\text{Pb}_{1-x}\text{Sr}_x(\text{Yb}_{1/2}\text{Nb}_{1/2})\text{O}_3$ system

S.B. Park ^{a,*}, W.K. Choo ^a, J.W. Park ^b

^aDepartment of Materials Science and Engineering, Korea Advanced Institute of Science and Technology, 373-1 Gusong-Dong, Yusong-Gu, Taejeon 305-701, South Korea

^bDevices and Materials Laboratory, LG Corporate Institute of Technology, Seoul 137-140, South Korea

Received 4 September 2000; received in revised form 2 November 2000; accepted 10 November 2000

Abstract

The crystal structure and dielectric properties of $\text{Pb}_{1-x}\text{Sr}_x(\text{Yb}_{1/2}\text{Nb}_{1/2})\text{O}_3$ (PSYN) system have been investigated by X-ray diffraction and dielectric measurement. The Curie temperature (T_c) of the solid solution does not change noticeably with the Sr content. At the same time, the maximum dielectric constant value gradually decreases with the increasing Sr concentration, and then finally the dielectric curve profile with respect to temperature becomes nearly flat. From the X-ray intensity studies of superlattices lines, it is deduced that Sr^{+2} ions hinder the antiparallel displacement of Pb^{+2} ions but their addition does not significantly affect the B-site ordering in $\text{Pb}(\text{Yb}_{1/2}\text{Nb}_{1/2})\text{O}_3$. © 2001 Published by Elsevier Science Ltd.

Keywords: Dielectric properties; Perovskites; Powders-solid state reaction; X-ray studies

1. Introduction

Lead ytterbium niobate, $\text{PbYb}_{1/2}\text{Nb}_{1/2}\text{O}_3$ (PYN) is one of the highly ordered complex perovskites that show paraelectric (PE) to antiferroelectric (AFE) transition near 302°C.^{1,2} The room temperature crystal structure of PYN was determined to be orthorhombic.^{1,2} $\text{SrYb}_{1/2}\text{Nb}_{1/2}\text{O}_3$ (SYN) is also the B-site ordered complex perovskite and shows nonferroelectric dielectric properties, and its room temperature crystal structure has been found to be monoclinic³ with its lattice parameters given as $a_m = 5.791$, $b_m = 5.822$, $c_m = 8.204$ Å and $\beta = 90.12^\circ$.

A-site cations play often an important role in phase transition.⁴ Especially, in case of lead-based perovskites of the multiple B-site $\text{Pb}(\text{B}', \text{B}'')\text{O}_3$, substitution of A-site cations causes severe changes in the crystal structure as well as in the dielectric properties as displayed by PLZT.⁵ Barium substituted PYN system also shows many changes in the crystal structure and the dielectric behavior.⁶ The high temperature phase of $\text{Pb}_{1-x}\text{Ba}_x(\text{Yb}_{1/2}\text{Nb}_{1/2})\text{O}_3$ ($0 \leq x \leq 0.3$) is still a B-site ordered

perovskite type of space group Fm3m with the doubled perovskite unit cell, which is characterized by the presence of superlattice peaks attributed to the ordering of Yb^{3+} and Nb^{5+} ions. But the low symmetry phase changes from a pseudo-cubic to an orthorhombic phase with the increasing Ba concentration. The dielectric behavior also changes from a sharp antiferroelectric phase transition to diffuse phase transition (DPT) with Ba substitution.

In the present work, we have investigated the crystal structure change that accompanies the Sr-substitution in PYN and its effect on the dielectric properties in $\text{Pb}_{1-x}\text{Sr}_x(\text{Yb}_{1/2}\text{Nb}_{1/2})\text{O}_3$. In this context the structural change and the associated phase transition at various compositions have been studied by X-ray powder diffraction and dielectric measurements.

2. Experimental

Polycrystalline ceramic samples were prepared by reacting the stoichiometric proportions of mixed high purity (99.9%) PbO , Yb_2O_3 , Nb_2O_5 and SrCO_3 powders. The powder mixture was ball-milled in acetone, dried and then calcined at 800–1000°C for 2 h. The calcined powders were reground, pressed and sintered at 1140–1280°C for 1 h in a controlled PbO atmosphere.

* Corresponding author. Tel.: +82-42-869-4253; fax: +82-42-869-4273.

E-mail address: azide@cais.kaist.ac.kr (S.B. Park).

Powder X-ray diffraction experiments of the sintered specimens after crushing and annealing have been carried out on a two-circle Rigaku Rotaflex X-ray diffractometer equipped with a curved graphite monochromator. Specimens for the dielectric investigations were electroded with silver paste by firing at 590°C for 5 min. The electrical capacitance and dielectric loss tangent were measured at several frequencies, between 1 kHz and 1 MHz, using a Hewlett Packard 4194A impedance/gain phase analyser while the test samples were heated at a constant 2°C/min rate.

3. Results and discussion

3.1. X-ray diffractions

Fig. 1 shows the X-ray diffraction patterns of $\text{Pb}_{1-x}\text{Sr}_x(\text{Yb}_{1/2}\text{Nb}_{1/2})\text{O}_3$ at room temperature at different Sr concentrations. For $0 \leq x \leq 0.3$, we have obtained single phase ceramics and above $x=0.3$ small amount of pyrochlore remained. For all the specimens studied, the superlattice diffraction patterns are comprised of two sets: reflection lines (marked by squares) due to the ordering of B-site cations on the octahedral position, and another set of superlattice lines (marked by circles) which indicate lead-cation displacements in antiferroelectric phase. It is the Pb displacement modulation that basically determines the PYN crystal structure. The modulation vector is $3/4 \ 3/4 \ 0$.²

The splitting of the fundamental reflections in the orthorhombic phase can be attributed to the slightly distorted monoclinic subcell from the prototype fcc cell. Using the indexing based on the prototype fcc unit cell,

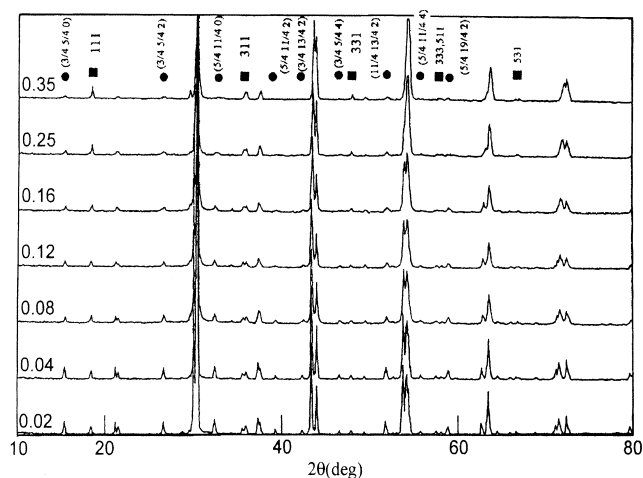


Fig. 1. The X-ray diffraction patterns of $\text{Pb}_{1-x}\text{Sr}_x(\text{Yb}_{1/2}\text{Nb}_{1/2})\text{O}_3$ system at room temperature: ■, superlattice reflections due to the B-site order; ●, superlattice reflections due to antiparallel cation displacements. The superlattice line indexing was done based on the prototype fcc unit cell $2a \times 2a \times 2a$, where a is the perovskite unit cell lattice parameter.

and from the $\{400\}$, $\{422\}$, $\{440\}$ and $\{620\}$ lines, the perovskite subcell lattice parameters, ($a = b, c$) and γ are calculated, where γ is the interaxial angle between the a - and b -axes.² The obtained results at room temperature are given in Fig. 2 as a function of the Sr composition. From the curves, the volume of subcell is found to decrease and both a and b gradually approach c with the increasing Sr concentration. This behavior is in contrast to that of $\text{Pb}_{1-x}\text{Ba}_x(\text{Yb}_{1/2}\text{Nb}_{1/2})\text{O}_3$ (PBYN) system.⁶ The substitution of atoms of different sizes causes volume expansion or contraction in addition to the chemical effect. In PBYN system, with the increasing of Ba composition, the unit cell volume increases since the ionic radius of Ba^{2+} (1.74 Å) is greater than that of Pb^{2+} (1.63 Å).⁷ Furthermore, the volume expansion due to Ba substitution induces the decrease in stability of the AFE phase. But in our system since the ionic radius of Sr^{2+} (1.54 Å) is smaller than that of Pb^{2+} , the unit cell volume decreases on substitution and the superlattice lines from the antiferroelectric phase remain in the whole composition range which we have studied.

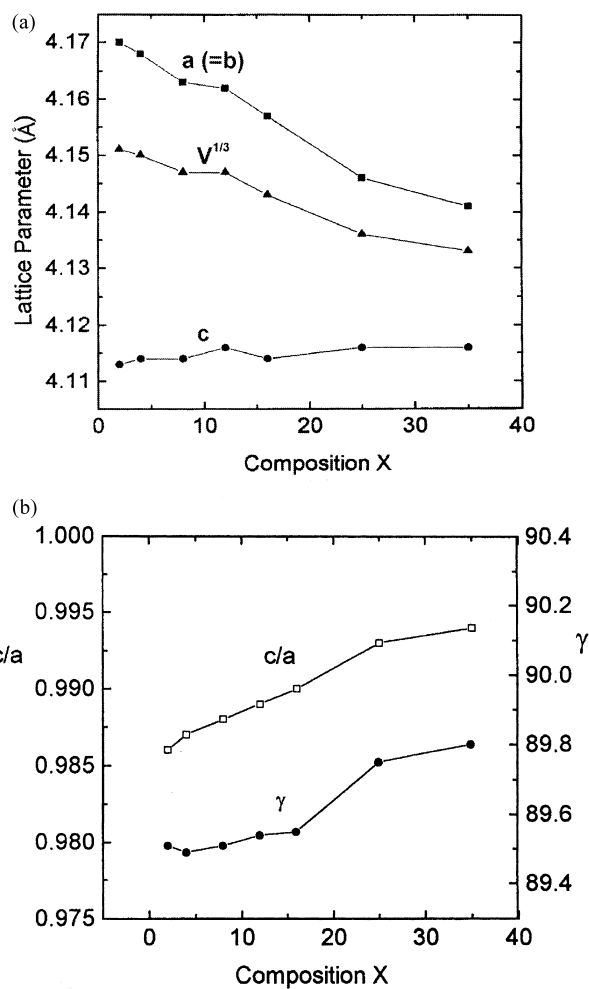


Fig. 2. Compositional dependence of the unit cell parameters of the $\text{Pb}_{1-x}\text{Sr}_x(\text{Yb}_{1/2}\text{Nb}_{1/2})\text{O}_3$ system as a function of temperature; (a) a , b and $V^{1/3}$ and (b) c/a , γ .

3.2. Dielectric properties

Fig. 3 shows the temperature dependence of the dielectric constant ϵ at 10 kHz at different Sr concentrations. For $0 \leq x \leq 0.2$, the temperature dependence of ϵ follows quite faithfully the Curie–Weiss law above T_c , and the general appearance is very similar to that of pure PYN. For $x > 0.2$, the dielectric constant vs. temperature curves become nearly flat and the behavior is apparently different from that of the lower concentration solutions. Because of such flattening behavior in dielectric curves, it becomes impossible to determine the transition temperature. In our system, the flattening of phase transition is different from the broadening of PBYN system. The diffuse transition in PBYN system is tied to a typical relaxor behavior. But in this case, as shown in Fig. 4(c), at $x = 0.35$, there is no perceptible frequency dependence of the dielectric constant as a

function of temperature. The flattening of phase transition and the lowering of the maximum dielectric constant can be explained by stabilization of the paraelectric state. As mentioned before, the unit cell volume contraction does not break the stability of antiferroelectric phase. But, as the degree of substitution of Sr atoms increases, the basically paraelectric nature of SYN establishes further and the Pb ions displacement decreases. As shown in Fig. 1, even though the superlattice lines by the Pb displacement exist in the whole composition range, their intensities evidently decrease. Therefore, if the Sr substitution increases more we can infer that the antiferroelectric phase disappears and the system may become paraelectric.

Fig. 5 shows the transition temperature variation as a function of the Sr compositions. The phase transition temperature decreases with increase in Sr substitution up to $x = 0.08$. For $0.08 < x \leq 0.2$, however, the transition

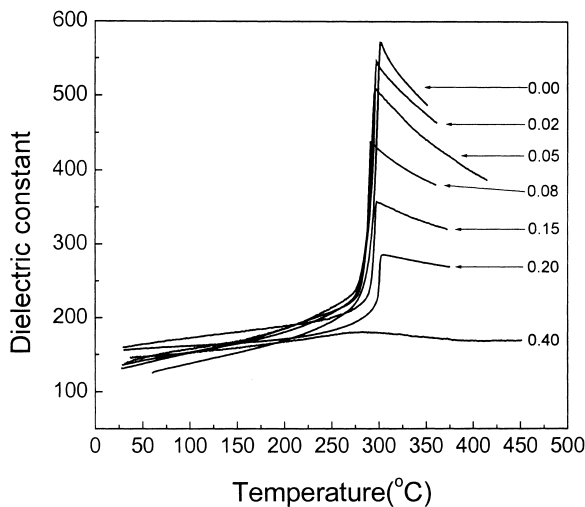


Fig. 3. Temperature dependence of the dielectric constants of $\text{Pb}_{1-x}\text{Sr}_x(\text{Yb}_{1/2}\text{Nb}_{1/2})\text{O}_3$ system at 10 kHz.

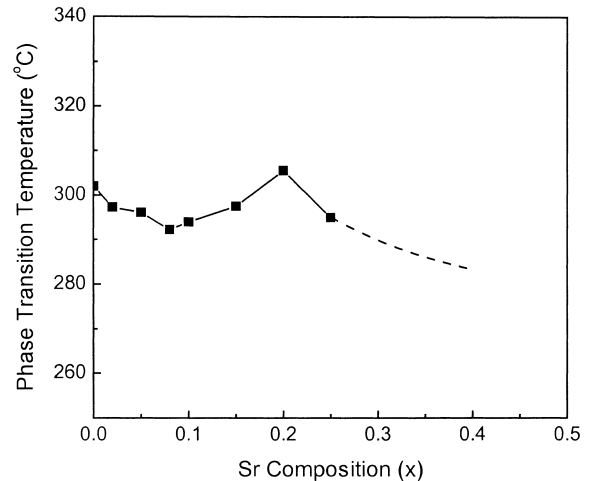


Fig. 5. Transition temperature change of $\text{Pb}_{1-x}\text{Sr}_x(\text{Yb}_{1/2}\text{Nb}_{1/2})\text{O}_3$ system as a function of x . The change occurring at $x \geq 0.25$ cannot be definitely determined.

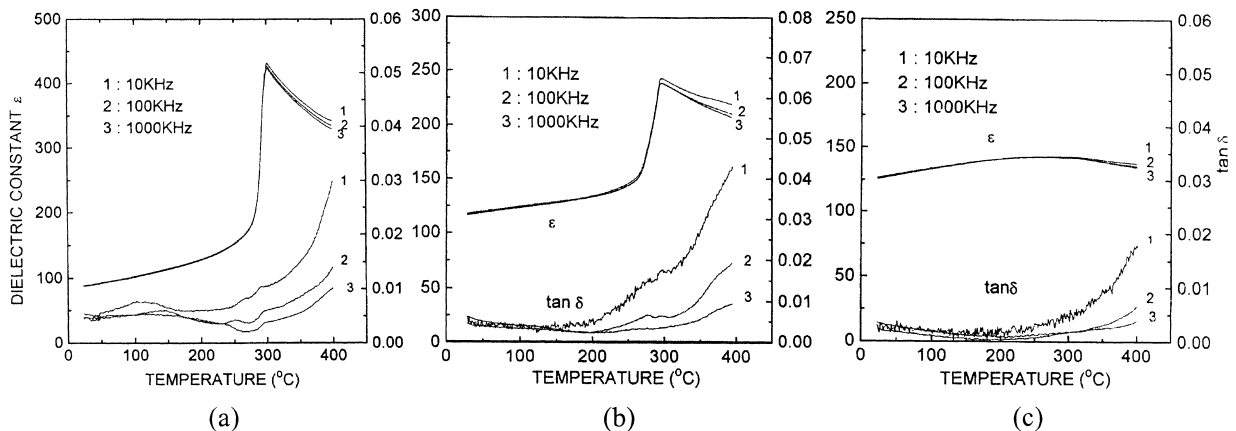


Fig. 4. Temperature dependence of the dielectric constant and $\tan \delta$ of $\text{Pb}_{1-x}\text{Sr}_x(\text{Yb}_{1/2}\text{Nb}_{1/2})\text{O}_3$ system at 10, 100, 1000 kHz; (a) $x = 0$, (b) $x = 0.16$, (c) $x = 0.35$.

temperature increases instead and finally for $x \geq 0.2$ it cannot be determined definitely but tends to decrease again. The change in the transition temperature is determined by the compromise between the unit cell volume and the polarizability effect of cations.⁸ In the PSYN solid solution, the ionic size of Sr^{2+} is smaller than that of Pb^{2+} and the electronic polarizability of Sr^{2+} ions is also smaller than that of Pb^{2+} . Therefore, if PSYN is a normal solid solution, its transition temperature would naturally decrease with Sr substitution like PBYN.⁶ But in the composition range $0.08 < x < 0.2$, the transition temperature increases slightly. A small initial Sr substitution should lower the transition temperature as the overall unit cell volume decreases and the Sr^{2+} content of smaller polarizability increases. But with a further decrease of the unit cell volume on additional Sr^{2+} substitution the space volume occupied by Pb^{2+} ions may decrease and the space volume occupied by Sr^{2+} is relatively larger than that of SYN. Therefore, we can infer that the polarizability of Pb^{2+} ions becomes smaller and the polarizability of Sr^{2+} increases and as a result the transition temperature increases slightly. Similar case can be found in $\text{Ca}_x\text{Ba}_{1-x}\text{TiO}_3$ system.⁸ For $x > 0.2$, because of large Sr substitution, the paraelectric state stabilizes and the transition temperature should decrease.

4. Conclusions

Our X-ray diffraction data shows that the superlattice lines attributed to B-site ordering and Pb-ion displacement remain throughout the whole composition range in of $\text{Pb}_{1-x}\text{Sr}_x(\text{Yb}_{1/2}\text{Nb}_{1/2})\text{O}_3$ we have investigated. The

phase transition temperature decreases with the increase in Sr substitution up to $x = 0.08$. For $0.08 < x \leq 0.2$, the transition temperature increases instead and finally for $x > 0.2$ the transition temperature decreases again. With large Sr substitution, $x \geq 0.3$, the dielectric constant curves vs. temperature flatten without a tendency toward frequency dispersions of the dielectric maximum temperature.

References

1. Poplavko, Y. M. and Tsykalov, V. G., Investigation of antiferroelectrics at millimeter wavelengths. *Sov. Phys. Solid State*, 1968, **9**, 2600–2603.
2. Kwon, J. R. and Choo, W. K., The antiferroelectric crystal structure of the highly ordered complex perovskite $\text{Pb}(\text{Yb}_{1/2}\text{Nb}_{1/2})\text{O}_3$, *J. Phys. Condens. Matter*, 1991, **3**, 2147–2155. Park, K. H. and Choo, W. K., Crystal structure and domain-wall orientations of antiferroelectric $\text{Pb}(\text{Yb}_{1/2}\text{Nb}_{1/2})\text{O}_3$. *J. Phys. Condens. Matter*, 1998, **10**, 5995–6007.
3. Yang, J. H., Choo, W. K., Lee, J. H. and Lee, C. H., The crystal structure of the B-site ordered complex perovskite $\text{Sr}(\text{Yb}_{1/2}\text{Nb}_{1/2})\text{O}_3$. *Acta Crystall.*, 1999, **B55**, 348–354.
4. Ter-Mikaelyan, G. B., Ivanov, S. A. and Venevtsev, Yu.N., An X-ray study of thermal atomic vibrations in oxygen-octahedra compounds. *Jpn. J. Appl. Phys.*, 1985, **24**(Suppl. 24–2), 603–605.
5. Haertling, G. H. and Land, C. E., Hot-pressed $(\text{Pb},\text{La})(\text{Zr},\text{Ti})\text{O}_3$ ferroelectric ceramics for electrooptic applications. *J. Am. Ceram. Soc.*, 1971, **54**, 1–11.
6. Kim, H. J., Park, K. H. and Choo, W. K., X-ray and electrical study of the phase transitions in $(\text{Pb}_{1-x}\text{Ba}_x)(\text{Yb}_{1/2}\text{Nb}_{1/2})\text{O}_3$. *Ferroelectrics*, 1992, **127**, 71–76.
7. Richerson, D. W., *Modern Ceramic Engineering: Properties, Processing, and Use in Design*, 2nd edn. Marcel Dekker, New York, 1992 (pp. 843–849).
8. Mitsui, T. and Westphal, W. B., Dielectric and X-ray studies of $\text{Ca}_x\text{Ba}_{1-x}\text{TiO}_3$ and $\text{Ca}_x\text{Sr}_{1-x}\text{TiO}_3$. *Phys. Rev.*, 1965, **124**, 1354–1359.